Rigid Fluorinated Polyimides with Well-Defined Polystyrene/ Poly(pentafluorostyrene) Side Chains from Atom Transfer Radical Polymerization

G. D. Fu, E. T. Kang,* and K. G. Neoh

Department of Chemical & Biomolecular Engineering, National University of Singapore, Kent Ridge, Singapore 119260

C. C. Lin and D. J. Liaw

Department of Chemical Engineering, National Taiwan University of Science and Technology, Taipei, Taiwan 106

Received March 28, 2005; Revised Manuscript Received June 30, 2005

ABSTRACT: Comb-shaped copolymers consisting of rigid fluorinated polyimide (FPI) backbone and well-defined polystyrene (PS) side chains (FPI-*cb*-PS), or poly(pentafluorostyrene) (PFS) side chains (FPI-*cb*-PFS), were synthesized by atom transfer radical polymerization (ATRP) from the bromide-containing FPI macroinitiators (FPI-Br). The sizes of the FPI-Br macroinitiators (consisting of 14 repeat units in the rigid backbone) and cleaved PS and PFS brushes (consisting of 35−144 and 32−93 repeat units, respectively) were estimated from the gel permeation chromatography (GPC) results. The lengths of the PS and PFS side chains determined from ^{1}H NMR spectroscopy were comparable to those determined from GPC or theoretical analysis. X-ray photoelectron spectroscopy (XPS) results confirmed the presence of grafted PS and PFS side chains on the respective FPI-*cb*-PS and FPI-*cb*-PFS copolymers as well as the presence of one ATRP bromide initiator per FPI repeat unit in the FPI-Br macroinitiator. Orderly arrays of the comb-shaped macromolecules, consisting of rigid FPI rods (backbones) of 20−30 nm in length and flexible PS brushes (side chains) of 4−6 nm in width, were imaged by atomic force microscopy (AFM). In addition to having a dielectric constant (κ) as low as 2.1, the resulting comb-shaped FPI-*cb*-PFS copolymer also exhibited good solution processability and good thermal stability (up to 470 °C).

1. Introduction

Recently, interest in the synthesis of polymers with specific molecular architectures has increased substantially.[1−4] Block,[5,6] graft,[7,8] star,[9−11] gradient,[12] hyperbranched,[13] and comb[14,15] polymers and copolymers have been synthesized by various radical and ionic polymerization techniques. These unique macromolecular architectures have allowed a wide range of applications, including stabilization of colloids, modification of crystal growth, controlling of micelle formation, and generation of intelligent materials for new drug carrier systems.[1]

Recent development in controlled free radical polymerizations, including atom transfer radical polymerization (ATRP), nitroxide-mediated radical polymerization (NMRP), and reversible addition−fragmentation chain transfer (RAFT) polymerization, has provided methodologies for synthesizing polymers in a controlled fashion, resulting in polymers with narrowly dispersed molecular weights.[4,16,17] The mechanism of living radical polymerization, which involves a rapid dynamic equilibrium between a minute amount of growing free radicals and a large majority of dormant species, can produce well-defined (nearly monodispersed) macromolecules with "active" or "living" chain ends. These "active" or "living" molecules can, in turn, be used to synthesize complex macromolecules with well-defined structure or architecture.[16]

Comb-shaped copolymers with densely grafted side chains can adopt the conformation of a cylindrical brush in a good solvent.[1] Such rodlike macromolecules are potentially useful for preparing molecular devices, such as molecular wires.[18] Comb-shaped polymers have been synthesized by living cationic polymerization[19,20] as well as by ATRP.[14,15,21]

Polyimides have been widely used as dielectric and encapsulation materials in microelectronics industry.[22−24] Methods for improving the dielectric, mechanical, and physicochemical properties of polyimides have included the incorporation of pendant fluoro- or perfluoroalkyl groups[25,26] and alteration of microstructure and morphology through block and graft copolymerizations.[27−32] The design and synthesis of fluoropolyimides with unique macromolecular architecture, high molecular weight, good thermal stability and solubility, and low dielectric constant remain of great interest. In this work, comb-shaped copolymers, consisting of fluorinated polyimide (FPI) backbones and polystyrene or poly(pentafluorostyrene) brushes, were synthesized by atom transfer radical polymerization from the FPI macroinitiators. The synthetic route is shown in Scheme 1. The resulting comb-shaped copolymers with rigid backbones (arising from the aromatic structure of polyimides) and nearly monodispersed polystyrene or poly(pentafluorostyrene) brushes were characterized by the gel permeation chromatography (GPC), NMR, X-ray photoelectron spectroscopy (XPS), thermal gravimetric analysis (TGA), atomic force microscopy (AFM), and dielectric constant measurements.

2. Experimental Section

2.1. Materials. 2,4-Dinitrophenol (97%), 4,4′-hexafluoroisopropylidene (99%), triethylamine (99.5%), tetrahydrofuran or

* To whom correspondence should be addressed. E-mail: cheket@nus.edu.sg.

10.1021/ma0506435 CCC: $30.25
Published on Web 08/12/2005

Scheme 1. Schematic Illustration of the Synthesis of Comb-Shaped Copolymers of Fluorinated Polyimide and Polystyrene (FPI-*cb*-PS) and of Fluorinated Polyimide and Polypentafluorostyrene (FPI-*cb*-PFS) by Atom Radical Polymerization (ATRP)

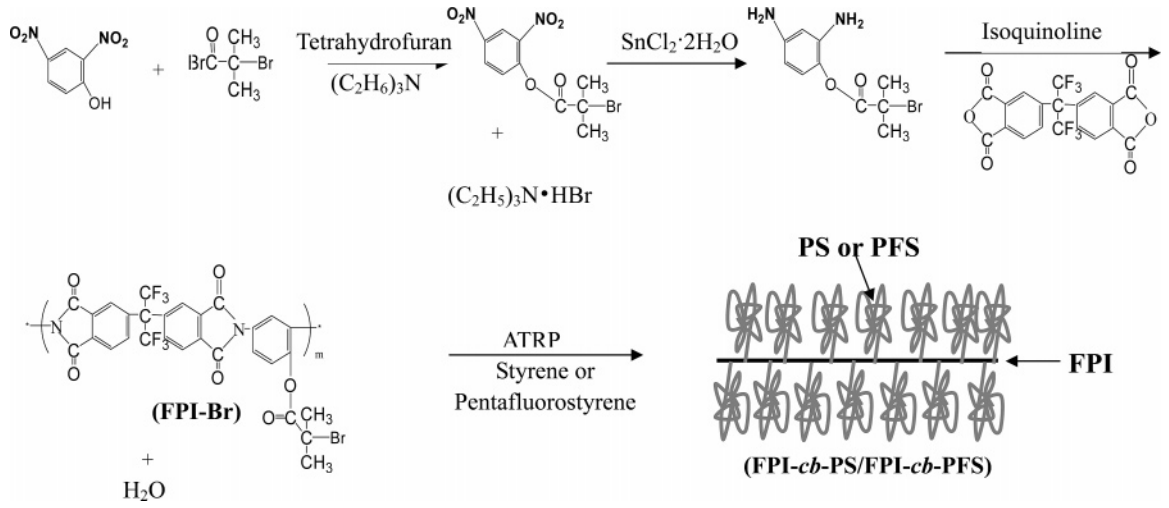

THF (Anal. Grade), and magnesium sulfate (99%) were purchased from Aldrich Chemical Co. of Sternheim, Germany. CuBr (99%), 2-bromoisobutyryl bromide (98%), $Sn^{II}Cl_2 \cdot 2H_2O$ (99.99%), ethyl acetate (Anal. Grade), methanol (Anal. Grade), *N,N,N′N′N′*-pentamethyldiethylenetriamine (PMDA, 99%), styrene (99%), and pentafluorostyrene (FS, 98%) were purchased from Aldrich Chemical Co. of Milwaukee, WI. 2,4-Dinitrophenol and 4,4′-hexafluoroisopropylidene were thoroughly dehydrated before use by heating at 80 °C under argon in an oven for 12 h. THF was dried by refluxing at 80 °C over sodium for 24 h. The styrene and FS monomers were passed through a ready-to-use disposable inhibitor removal column (Aldrich Chem. Co.) prior to use.

2.2. Chemical Synthesis. 2.2.1. Synthesis of 2,4-Dinitrophenyl-2-bromoisobutyryate. 2,4-Dinitrophenol (3.0 g, 16 mmol), triethylamine (2.8 mL, 20 mmol), and THF (40 mL) were introduced into a 100 mL three-neck round-bottom flask equipped with a condenser, a dropping funnel, and a nitrogen inlet/outlet. After cooling to 0 °C, 2-bromoisobutyryl bromide (5.0 mL, 41 mmol) in 10 mL of THF was added slowly, with continuous stirring, to the mixture over a period of 1 h under a nitrogen atmosphere. The temperature was allowed to rise to room temperature. The reaction stirred for 24 h. The $(C_2H_5)_3N \cdot HBr$ was removed by filtration and the solvent removed by rotary evaporation. The product was isolated as an orange brown liquid, which crystallized upon standing. The solid was washed three times with 20 mL of ethanol to give a pale yellow crystalline product. Yield = 48%; mp: 79 °C (DSC). ^{1}H NMR ($CDCl_3$, δ/ppm): 8.98 (d, 1H, aromatic ring), 8.57 (dd, 1H, aromatic ring), 7.59 (d, 1H, aromatic ring) and 2.10 (s, 6H, CH_3). ^{13}C NMR ($CDCl_3$, δ/ppm): 168.44 (C=O), 148.27 (aromatic ring), 145.33 (aromatic ring), 141.50 (aromatic ring), 129.16 (aromatic ring), 126.11 (aromatic ring), 121.74 (aromatic ring), 53.96 (C−Br), and 30.25 (CH_3). FTIR (solid, ATR cell): 1335 cm^{-1} (NO_2) and 1760 cm^{-1} (C=O).

2.2.2. Synthesis of 2,4-Diaminophenyl-2-bromoisobutyrate. 2,4-Dinitrophenyl-2-bromoisobutyrate (5.0 g, 15 mmol) and $SnCl_2 \cdot 2H_2O$ (33.9 g, 150 mmol) were dissolved in 200 mL of ethyl acetate. The mixture was refluxed for 1 h at 80 °C and cooled, and the pH was adjusted to 8−9 using a 5 wt % aqueous solution of sodium bicarbonate. Distilled water (200 mL) was added to separate the ethyl acetate layer. The organic layer was washed with saturated brine solution (3 × 200 mL), followed by distilled water (2 × 200 mL). The organic layer was then dried with magnesium sulfate, and the solvent was removed under reduced pressure. A light brown crystalline product was obtained. The product was purified by column chromatography with ethyl acetate as the mobile phase. Yield = 55%; mp > 200 °C. ^{1}H NMR ($CDCl_3$, δ/ppm): 7.27 (d, 1H, aromatic ring), 6.63 (d, 1H, aromatic ring), 6.26 (dd, 1H, aromatic ring), 4.56 (s, 4H, NH_2) and 2.01 (s, 6H, CH_3). ^{13}C NMR ($CDCl_3$, δ/ppm): 168.55 (C=O), 140.97 (aromatic ring), 138.04 (aromatic ring), 126.01 (aromatic ring), 115.70 (aromatic ring), 110.52 (aromatic ring), 107.26 (aromatic ring), 62.18 (C−Br), and 31.43 (CH_3). FTIR (solid, ATR cell): 3341, 3283 cm^{-1} (NH_2) and 1666 cm^{-1} (C=O).

2.2.3. Synthesis of the Fluorinated Polyimide Macroinitiators. Initially, 0.41 g of 2,4-diaminophenyl-2-bromoisobutyrate (1.5 mmol) was dissolved in 3 mL of freshly distilled *m*-cresol. Then, 4,4′-hexafluoroisopropylidene (6FDA) (0.666 g, 1.50 mmol) and isoquinoline (0.4 mL, as the catalyst) were added at room temperature under a nitrogen atmosphere. The mixture was stirred for 1 h at room temperature. The temperature was slowly raised to 160 °C and refluxed for 18 h. The polymerization was performed under flowing nitrogen to remove the water produced during imidization. The resulting viscous solution was poured into 100 mL of methanol with stirring. The precipitate was removed by filtration. The fluorinated polyimide macroinitiators (FPI-Br) so obtained were washed twice with 20 mL of methanol and then hexane, before being dried at 100 °C for 12 h under reduced pressure. Yield = 42%. FTIR (solid, ATR cell): 1781, 1713 cm^{-1} (C=O), and 1366 cm^{-1} (C−N). $M_n = 9.4 \times 10^3$ g/mol and polydispersity index (PDI = M_w/M_n) = 1.31, from gel permeation chromatography (GPC).

2.2.4. Comb-Shaped Copolymers via ATRP. (a) In a typical copolymerization reaction, 0.067 g (0.007 mmol) of FPI-Br was dissolved in 0.2 mL of DMF. Then, 14.3 mg (0.10 mmol) of CuBr, 0.02 mol of styrene, and 0.01 mmol of PMDA were added. After three freeze−evacuate−thaw cycles, the mixture was heated to 110 °C for 120 min. The reaction mixture was diluted with THF, eluted through an alumina column to remove the copper complex, and then poured into 200 mL of methanol to induce precipitation of the copolymer. The comb-shaped copolymer with the FPI backbone and polystyrene (PS) brushes (side chains) is referred to as the FPI-*cb*-PS copolymer. About 0.49 g of white powders was obtained ($M_n = 6.6 \times 10^4$ g/mol and PDI = 1.41 from GPC).

(b) In another copolymerization reaction, 0.067 g of FPI-Br was dissolved in 0.2 mL of DMF. Then, 14.3 mg (0.1 mmol) of CuBr, 0.02 mol of pentafluorostyrene, and 0.01 mmol of PMDA were added. After three freeze−evacuate−thaw cycles, the mixture was heated to 110 °C for 120 min. The reaction mixture was diluted with THF, eluted through an alumina column to remove the copper complex, and then poured into 200 mL of methanol to induce the precipitation of the copolymer. The comb-shaped copolymer with the FPI backbone and poly(pentafluorostyrene) (PFS) brushes (side chains) is referred to as the FPI-*cb*-PFS copolymer. About 0.77 g of pale brown powders was obtained ($M_n = 7.8 \times 10^4$ g/mol and PDI = 1.46 from GPC).

2.2.5. Cleavage of Side Chains from the Comb-Shaped Copolymers. In a typical reaction, 0.2 g of the FPI-*cb*-PS copolymer ($M_n = 6.6 \times 10^4$ g/mol and PDI = 1.41 from GPC) was dissolved in a mixture of 20 mL of 5 wt % methanol solution of KOH and 30 mL of THF in a 100 mL round-bottom flask. The reaction mixture was refluxed for 1 week. When the solution was cooled to room temperature, concentrated hydrochloric acid was added to adjust the pH value to about 7. The mixture was extracted with chloroform and washed with water. The solvent was evaporated under reduced pressure. The remaining solid was dried by pumping under reduced pressure at room temperature. About 0.14 g of white powders was obtained ($M_n = 3.7 \times 10^3$ g/mol and PDI = 1.41 from GPC).

2.3. Materials Characterization. The structures of the FPI-Br and the comb-shaped copolymers were characterized by ^{1}H NMR spectroscopy on a Bruker ARX 300 MHz spectrometer. $CDCl_3$ was used as the solvent for the FPI-Br and FPI-*cb*-PS copolymers. For the FPI-*cb*-PFS copolymers, tetrahydrofuran-d_8 was used instead. Gel permeation chromatography (GPC) was performed on an HP 1100 HPLC, equipped with a HP 1047A refractive index detector and a PLgel MIXED-C 300 × 7.5 mm column (packed with 5 μm particles of different pore sizes). The column packing allowed the separation of polymers over a wide molecular weight range of 200−3 000 000. THF was used as the eluent at a flow rate of 1 mL/min at 35 °C. Polystyrene standards were used as the references. Thermal properties of the copolymers were measured by thermal gravimetric analysis (TGA). The samples were heated to 900 °C at a heating rate of 10 °C/min under a dry nitrogen atmosphere in a Du Pont Thermal Analyst 2100 system, equipped with a TGA 2050 thermal gravimetric analyzer. Differential scanning calorimetry (DSC) studies were conducted on a DSC82ze apparatus (Mettler Toledo Co., Zurich, Switzerland) at a heating rate of 10 °C/min under a nitrogen atmosphere. FTIR measurements were carried out on a Bio-Rad FTS 165 spectrophotometer by dispersing the sample in an ATR cell. XPS measurements were carried out on a Kratos AXIS HSi spectrometer (Kratos Analytical Ltd., Manchester, England) with a monochromatized Al Kα X-ray source (1486.6 eV photons). The X-ray source was run at a reduced power of 150 W (15 kV and 10 mA). The samples were mounted on the standard sample studs using double-sided adhesive tapes. The core-level spectra were obtained at a photoelectron takeoff angle (with respect to the sample surface) of 90°. The pressure in the analysis chamber was maintained at 10^{-8} Torr or lower during sample measurements. The dielectric constants (κ's) of the copolymer films were measured on a RF impedance/capacitance material analyzer (Hewlett-Packard model 4291B) in the frequency range of 1 MHz−1.8 GHz and at 50% relative humidity (25 °C) under an ambient atmosphere. Each film for dielectric constant measurement was obtained by spin-coating from a 10 wt % THF solution of the comb-shaped copolymer on a clean Si(100) substrate at 1000 rpm. The film so-obtained had a thickness in the range of 10−20 μm, depending on the molecular weight of the copolymer. Film density was measured on a top-loading electronic Mettler Toledo balance (model AP250D, equipped with a density kit) according to the Archimedean principle. The mechanical properties of the polymer and copolymer film were measured on an Instron model 5544 tensile tester from Instron Corp.

2.4. Macromolecular Structure of the Comb-Shaped Copolymers. About 0.01 g of the FPI-*cb*-PS copolymer ($M_n = 1.4 \times 10^5$ g/mol) was dissolved in 50 mL of THF. The solution was spin-coated on a hydrogen-terminated Si(100) substrate (Si−H substrate) at 2000 rpm until the solvent had evaporated completely. The Si−H substrate was obtained by etching of the oxide-covered Si(100) substrate with 10 vol % HF. In comparison with the hydrophilic nature of the oxide-covered silicon surface, the hydrophobic nature of the Si−H surface allowed better interactions of the hydrophobic copolymer with the substrate surface. The surface morphology of the film was studied by AFM, using a Nanoscope IIIa AFM from the Digital Instruments Inc. In each case, an area of 500 nm × 500 nm was scanned using the tapping mode. The drive frequency was 330 ± kHz, and the voltage was between 3.0 and 4.0 V. A drive amplitude of 300 mV, a set point of 3.34 μV, and a scan rate of 1.0 Hz were used.

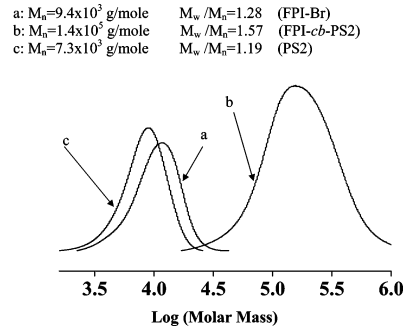

Figure 1. Gel permeation chromatography (GPC) traces of the (a) bromide-containing fluorinated polyimide macroinitiator (FPI-Br), (b) comb-shaped copolymer of fluorinated polyimide and polystyrene (FPI-*cb*-PS2 in Table 1; synthetic conditions: [styrene]:[Br]$_{FPI-Br}$:[CuBr]:[PMDA] = 200:1:1:1 at 110 °C for 4 h, PMDA = *N*,*N*,*N*′*N*′*N*′-pentamethyldiethylenetriamine), and (c) polystyrene (PS) side chains hydrolyzed from FPI-*cb*-PS2.

3. Results and Discussion

3.1. Graft Copolymerization of Styrene and Pentafluorostyrene from the FPI Macroinitiators. The process of synthesizing the comb-shaped copolymers of fluorinated imide and styrene (or pentafluorostyrene) is shown schematically in Scheme 1. Initially, 2,4-diaminophenyl-2-bromoisobutyrate was synthesized by the reduction of 2,4-dinitrophenyl-2-bromoisobutyrate. The latter was prepared from the reaction of 2,4-dinitrophenol with 2-bromoisobutyric acid. The fluorinated polyimide (FPI) macroinitiators (FPI-Br) were prepared from 2,4-diaminophenyl-2-bromoisobutyrate and 4,4′-hexafluoroisopropylidene by a one-step condensation reaction. 4,4′-Hexafluoroisopropylidene was used because the resulting polymer had relatively good solubility in common organic solvents, such as THF and DMF.[22] The FPI-Br macroinitiator should be completely imidized to prevent the carboxylic group from reacting with the Cu(II) species of the atom radical polymerization (ATRP) catalyst system. The reaction led to the formation of metal carboxylates which could inhibit deactivation in ATRP.[33]

The pristine FPI-Br has a number-average molecular weight (M_n) of about 9.4×10^3 g/mol (corresponding to an average of 14 repeat units), weight-average molecular weight (M_w) of about 1.2×10^4 g/mol, and a polydispersity index (PDI = M_w/M_n) of about 1.31, as indicated by gel permeation chromatography (GPC) results of Figure 1 (trace a). Trace b shows the GPC results of a comb-shaped copolymer of FPI and polystyrene (FPI-*cb*-PS copolymer) from a monomer (styrene) to initiator molar feed ratio of 200 and a reaction time of 4 h (sample FPI-*cb*-PS2 in Table 1). After the ATRP of styrene, the M_n of the resulting FPI-*cb*-PS2 copolymer increases dramatically to 1.4×10^5 g/mol, and PDI of the copolymer also increases to 1.57. Trace c is the GPC result of the PS side chains, cleaved from the FPI-*cb*-PS2 copolymer. The side chains have a M_n of about 7.3×10^3 (containing about 70 repeat units of styrene) and a PDI of about 1.19. GPC results of the copolymers prepared from other reaction time are also summarized in Table 1. The increase in PDI of the FPI-*cb*-PS copolymer from that of the starting FPI-Br can be attributed to the fact that there are more initiator sites

Table 1. Characterization of the Fluorinated Polyimide (FPI) and Polystyrene (PS)/Poly(pentafluorostyrene) (PFS) Copolymers

									PS/PFS brushes of the copolymers				
sample	monomer conv (%)	reaction time (min)	M_n[a] (g/mol)	PDI[b]	M_n[c] (g/mol)	M_n[d] (g/mol)	density[e] (g/cm^3)	κ	M_n[a,f] (g/mol)	PDI[b]	styrene or FS repeat units[f]	styrene or FS repeat units[c]	styrene or FS repeat units[d]
FPI-Br			9.4×10^3 [g]	1.31			1.41	3.0					
FPI-*cb*-PS1[h]	20	120	6.6×10^4	1.41	6.9×10^4	6.8×10^4	1.10	2.6	3.7×10^3	1.14	35	41	40
FPI-*cb*-PS2[h]	34	240	1.4×10^5	1.57	1.0×10^5	1.1×10^5	1.04	2.6	7.3×10^3	1.19	70	62	68
FPI-*cb*-PS3[h]	70	600	2.6×10^5	1.64	2.3×10^5	2.1×10^5	1.00	2.5	1.5×10^4	1.13	144	151	140
FPI-*cb*-PFS1[h]	18	120	7.8×10^4	1.46	1.0×10^5	1.1×10^5	1.33	2.2	6.2×10^3	1.16	32	35	36
FPI-*cb*-PFS2[h]	35	240	1.6×10^5	1.54	1.8×10^5	2.0×10^5	1.30	2.1	9.8×10^3	1.15	51	64	70
FPI-*cb*-PFS3[h]	74	600	3.6×10^5	1.71	3.7×10^5	4.3×10^5	1.30	2.1	1.8×10^4	1.21	93	132	148

[a] Determined from gel permeation chromatography (GPC) using polystyrene standards as references. [b] PDI = number molecular weight (M_n)/weight-average molecular weight (M_w). [c] Calculated from ^{1}H NMR spectroscopy results. [d] Theoretical values calculated from conversion data. [e] Determined according to the Archimedean principle. Density of PS = 1.05 g/cm^3, density of PFS = 1.43 g/cm^3. [f] Cleaved side chains from hydrolysis of the corresponding copolymer (FS = pentafluorostyrene). [g] Corresponding to about 14 repeat units. [h] The copolymer was synthesized using the bromide-containing fluorinated polyimide macroinitiator (FPI-Br). The molar feed ratio of [styrene (or pentafluorostyrene)]:[Br]FPI-Br:[CuBr]:[PMDA] = 200:1:1:1 (PMDA = *N,N,N′N′N′*-pentamethyldiethylenetriamine).

in the fraction of FPI macroinitiator with a higher molecular weight. Thus, after graft copolymerization with styrene, the large molecules will become even larger, leading to a wider distribution in molecular sizes of the resulting copolymers. The ATRP of pentafluorostyrene (FS) from the FPI macroinitiators produced the corresponding FPI and poly(pentafluorostyrene) copolymer (FPI-*cb*-PFS copolymer). At the given monomer-to-initiator molar feed ratio of 200:1 and at a polymerization time of about 2 h, the M_n of the FPI-*cb*-PFS copolymer increases markedly form 9.4×10^3 to 7.8×10^4. At the same time, the PDI increases from 1.31 to 1.46 (sample FPI-*cb*-PFS1 in Table 1). The increase in PDI is similar to that observed in the FPI-*cb*-PS copolymers. Table 1 also shows that, with the increase in reaction time, the conversion of monomer also increases. The theoretical M_n's of the comb-shaped FPI-*cb*-PS and FPI-*cb*-PFS copolymers (6.8×10^4 to 2.1×10^5 g/mol and 1.1×10^5 and 4.3×10^5 g/mol, respectively, for ATRP reaction time of 2−10 h) calculated from their respective monomer conversions are in reasonable agreement with those obtained from GPC measurements.

The length of PS (or PFS) side chains in the FPI-*cb*-PS (or FPI-*cb*-PFS) copolymers can be regulated by varying the reaction time at the given monomer-to-initiator feed ratio (200:1). Table 1 shows the GPC results of the cleaved PS and PFS side chains from the FPI-*cb*-PS and FPI-*cb*-PFS copolymers, respectively. As the reaction time increased from 120 to 600 min, the M_n of the PS side chains increased from 3.7×10^3 to 1.5×10^4 g/mol, while the PDI remained at around 1.2. For the corresponding FPI-*cb*-PFS copolymers, the M_n of the PFS side chains increased from 6.2×10^3 to 1.8×10^4 g/mol, and the PDI remained at around 1.2. The results indicate that comb-shaped FPI-*cb*-PS and FPI-*cb*-PFS copolymers with fairly well-defined, or narrowly dispersed, PS and PFS side chains have been synthesized from the FPI-Br macroinitiators by ATRP. For the FPI-*cb*-PFS copolymers prepared under a prolonged ATRP time (for example, FPI-*cb*-PFS3 in Table 1), the M_n and the length of the cleaved PFS side chains obtained from GPC were lower than those determined from NMR spectroscopy and/or theoretical calculations. The discrepancy probably arose form the difference in hydrodynamic volumes between FPI-*cb*-PFS (or PFS) and the PS standards used as GPC references.

3.2. Chemical Structures of the FPI-Br Macroinitiators and the FPI-*cb*-PS and FPI-*cb*-PFS Copolymers. The chemical structures of the FPI-Br macroinitiators and the FPI-*cb*-PS copolymers were studied by ^{1}H NMR spectroscopy. Figure 2a shows the ^{1}H NMR spectrum of the FPI-Br macroinitiators described in Table 1. The chemical shifts at about 1.8 ppm and in the range of 6.4−8.2 ppm are attributable to the protons of the bromo esters and aromatic protons of the FPI, respectively. The minor chemical shifts in the range of 2.0−4.1 ppm are probably associated with *sec*-butyl ($-(CH_3)_2CH$) or hydroxyl (OH) groups incorporated during the FPI synthesis. Figure 2b shows the ^{1}H NMR spectrum of a FPI-*cb*-PS copolymer (sample FPI-*cb*-PS2 in Table 1). The chemical shifts in the range of 6.3−8.2 ppm are attributable to the aromatic protons of FPI and the PS side chains. Grafting of PS from FPI has resulted in the appearance of chemical shifts in the range of 1.6−2.4 ppm, attributable to the aliphatic $-CH-CH_2-$ of the PS side chains. The chemical shift at about 1.2 ppm is attributable to the $C-CH_3$ group, while the chemical shift at about 4.4 ppm is associated with the $-CH$Br terminal group. The average length of PS side chains in the FPI-*cb*-PS copolymer can also be determined from the ^{1}H NMR spectrum, using the area of the methylidyne protons in the $-CH$Br terminal group (**k** in Figure 2b) and the areas of the methylene and methylidyne protons (**i** and **j** in Figure 2b) in the backbone of the PS side chain. The NMR-derived copolymer compositions are also given in Table 1. The average length of the PS side chains deduced from NMR results is in reasonably good agreement with that estimated from GPC results.

Figure 2c shows the ^{1}H NMR spectrum of a FPI-*cb*-PFS copolymer (sample FPI-*cb*-PFS2 in Table 1). The chemical shifts in the range of 6.3−8.2 ppm are attributable to the aromatic protons of the FPI. Grafting of PFS side chains to FPI has resulted in the appearance of chemical shifts in the range of 2.0−2.9 ppm, attributable to the aliphatic $-CH-CH_2-$ of the PFS side chains. The chemical shift at about 1.1 ppm is attributable to the $C-CH_3$ group, while the chemical shift at about 4.8 ppm is associated with the $-CH$Br terminal group. The average length of the PFS side chains in the FPI-*cb*-PFS copolymer can also be determined from the ^{1}H NMR spectrum, using the area of the methyl protons in the bromoester group (**g** in Figure 2c) and the areas of the methylene and methylidyne protons (**i** and **j** in

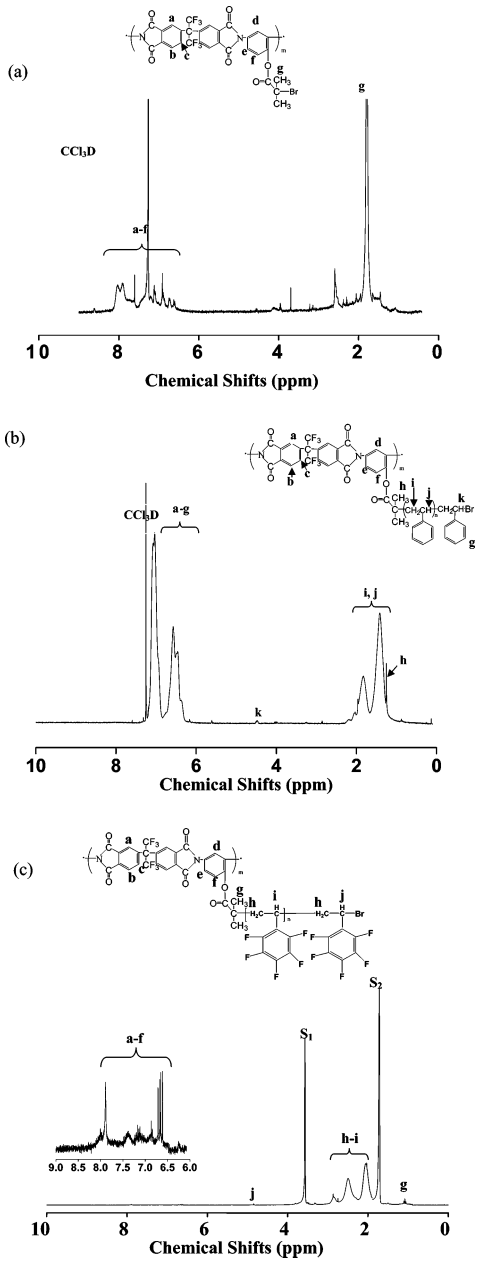

Figure 2. 300 MHz ^{1}H NMR spectra of the (a) bromide-containingd fluorinated polyimide macroinitiator (FPI-Br) having a M_n of about 9.4 × 10^3 g/mol, (b) comb-shaped copolymer of fluorinated polyimide and polystyrene (FPI-*cb*-PS2 in Table 1; synthesis conditions: [styrene]:[Br]$_{FPI-Br}$:[CuBr]:[PMDA] = 200:1:1:1 at 110 °C for 4 h, PMDA = *N,N,N′N′N′*-pentamethyldiethylenetriamine) having a M_n of about 1.4 × 10^5 g/mol, and (c) comb-shaped copolymer of fluorinated polyimide and polypentafluorostyrene (FPI-*cb*-PFS2 in Table 1; synthesis conditions: [PF]:[Br]$_{FPI-Br}$:[CuBr]:[PMDA] = 200:1:1:1 at 110 °C for 4 h) having a M_n of about 1.6 × 10^5 g/mol.

Figure 2c) in the backbone of the PFS side chain. The average chain length of PFS in each copolymer, deuced from NMR results, is also given in Table 1. Again, the average length of PFS side chains obtained from the NMR results is in reasonable agreement with that estimated from the GPC results.

3.3. Chemical Composition of the FPI-Br Macroinitiators and the FPI-*cb*-PS and FPI-*cb*-PFS Copolymers. Figure 3 shows the respective C 1s and Br 3d core-level spectra of (a) the FPI-Br macroinitiators and (b) the FPI-*cb*-PS copolymer (FPI-*cb*-PS2 in Table

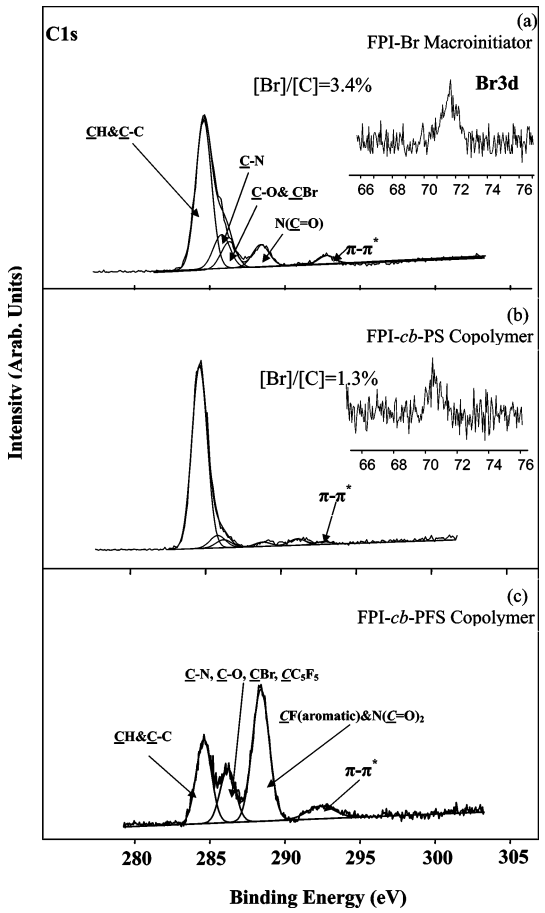

Figure 3. C 1s and Br 3d core-level spectra of the (a) bromide-containing fluorinated polyimide macroinitiator (FPI-Br) having a M_n of about 9.4 × 10^3 g/mol, (b) comb-shaped copolymer of fluorinated polyimide and polystyrene (FPI-*cb*-PS2 in Table 1; synthesis conditions: [styrene]:[Br]$_{FPI-Br}$:[CuBr]:[PMDA] = 200:1:1:1 at 110 °C for 4 h, PMDA = *N,N,N′N′N′*-pentamethyldiethylenetriamine) having a M_n of about 1.4 × 10^5 g/mol, and (c) comb-shaped copolymer of fluorinated polyimide and polypentafluorostyrene (FPI-*cb*-PFS2 in Table 1; synthesis conditions: [PF]:[Br]$_{FPI-Br}$:[CuBr]:[PMDA] = 200:1:1:1 at 110 °C for 4 h) having a M_n of about 1.6 × 10^5 g/mol.

1). The C 1s core-level spectrum of the FPI-Br macroinitiators can be curve-fitted with five peak components, having binding energies (BE's) at 284.6 eV for the *C*−H species, at 285.8 eV for the *C*−N, at 286.2 eV for the *C*−O species, at 288.4 eV for the N(*C*═O)$_2$ species, and at 292.8 eV for the *C*F$_3$ species.[34] The BE of the *C*−Br species at about 286.3 eV[35] overlaps with that of the *C*−O species. The BE's of the O−*C*═O species and the N(*C*═O) imide species cannot be resolved unambiguously. The two species are represent by a single peak component at the BE of about 288.4 eV. The XPS-derived [Br]/[C] ratio of 0.034 in Figure 3a for the FPI-Br macroinitiators is comparable to the theoretical ratio of 0.035, based on the chemical structure of FPI-Br. Thus, there is approximately one bromide group (grafting site) per repeat unit of PFI.

The substantial increase in intensity of the *C*−H peak component at the BE of 284.6 eV and the appearance of the $\pi-\pi^*$ shake-up satellite at the BE of 291.1 eV in Figure 3b are consistent with the presence of the PS side chains in the FPI-*cb*-PS copolymer. The intensity of the Br 3d core-level signal in the FPI-Br macroinitiators has decreased substantially after the ATRP of styrene because the relative concentration of Br in the FPI-*cb*-PS copolymer is lower than that of Br in the FPI-

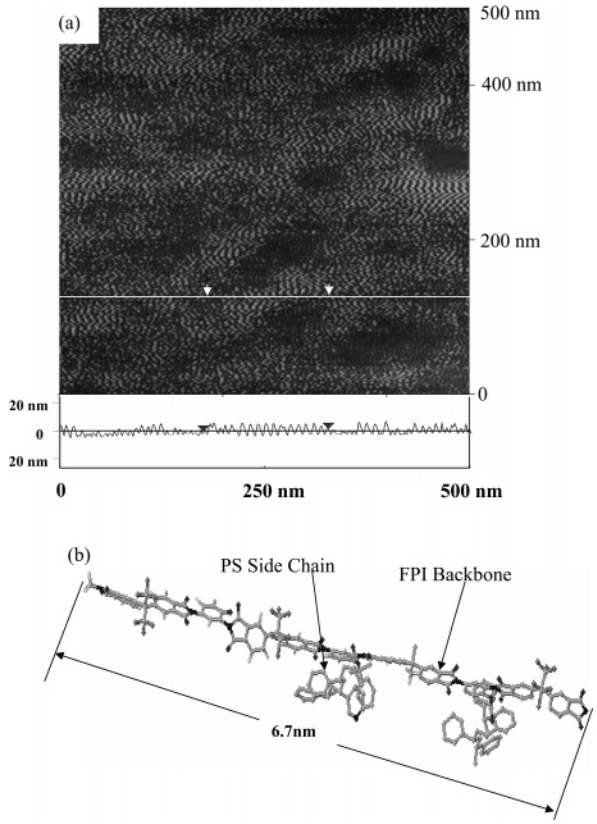

Figure 4. (a) AFM image of the macromolecular assembly of comb-shaped copolymer of fluorinated polyimide and polystyrene (FPI-*cb*-PS2 in Table 1; synthesis conditions: [styrene]:$[Br]_{FPI-Br}$:[CuBr]:[PMDA] = 200:1:1:1 at 110 °C for 4 h, PMDA = *N,N,N′N′N′*-pentamethyldiethylenetriamine) on a hydrogen-terminated Si(100). The overall size of the image is approximately 500 nm × 500 nm. The topographical roughness of the surface with self-assembled macromolecular arrays is also shown. (b) A comb-shaped copolymer model of fluorinated polyimide and polystyrene (FPI-*cb*-PS) having 4 imide repeat units in the main chain and 2 PS side chains with 4 styrene repeat units each.

Br macroinitiators. The C 1s core-level spectrum (Figure 3c) of the FPI-*cb*-PFS copolymer (FPI-*cb*-PFS2 in Table 1) can be curve-fitted with four peak components, having BE's at 284.6 eV for the *C*−H species, at 286.1 eV for the $-CC_5F_5$ species, at 288.4 eV for the *C*F(aromatic) species, and at 292.4 eV for the $\pi-\pi^*$ shake-up satellite.[35] The BE's of the *C*−Br species at about 286.3 eV and the *C*−O species at about 286.2 eV overlap with that of the CC_5F_5 species (286.1 eV). The BE's of the O−*C*═O species and the N(*C*═O)$_2$ imide species cannot be resolved unambiguously from that of the *C*F(aromatic) species.

3.4. AFM Characterization of the Comb-Shaped FPI Copolymers. The comb-shaped FPI copolymers were further characterized by atomic force microscopy (AFM). Figure 4a shows an AFM tapping mode image of the FPI-*cb*-PS copolymer (FPI-*cb*-PS2 in Table 1) on a hydrogen-terminated silicon (Si−H) surface. The latter is more hydrophobic than the pristine (oxide-covered) silicon surface[35] and is expected to improve the interaction with the hydrophobic FPI-*cb*-PS macromolecules. Microdomains of orderly aligned rigid macromolecular chains are discernible from the AFM image. The FPI-*cb*-PS molecules were found to self-assemble or align on the Si−H surface. The orderly assembly of the FPI-*cb*-PS molecules probably has resulted from the stiffness of the FPI backbone arising from the rigid conformation of aromatic rings. The excluded volumes of dense side chains forced the comb-shaped FPI-*cb*-PS macromolecules to assume a rodlike conformation in a good solvent, e.g., THF. When the dilute THF solution of FPI-*cb*-PS was cast onto a "compatible" substrate, the rodlike copolymers self-assembled on the Si−H surface into ordered macromolecular arrays to minimize the surface energy.

With a M_n of about 1.4×10^5 g/mol, each molecule of FPI-*cb*-PS2 has, on the average, about 14 repeat units of the fluorinated imide in its backbone and 70 styrene units in each of its 14 side chains. Figure 4b shows the 3-dimensionally optimized state[37] of a FPI-*cb*-PS copolymer molecule with 4 FPI repeat units in the backbone and 2 PS side chains, each with 4 styrene repeat units. The PS side chain exists as random coil and has a dimension of about 1 nm. Arising from the rigidity of the aromatic rings, the FPI backbone with 4 FPI repeat units has a fully extended length of about 6.7 nm in the presence of torsion among the aromatic rings.

In the AFM image of Figure 4a, the rigid-rod-like FPI-*cb*-PS2 macromolecules have lengths in the range of 20−30 nm and widths in the range of 4−6 nm. Since each FPI repeat unit has a calculated length of about 1.7 nm, the observed length of the FPI-*cb*-PS2 backbone (∼14 repeat units) is comparable to that of the theoretical dimension (24 nm). As for the PS side chains, they probably exist as random coils around the rigid FPI backbone. The width or the radius of the FPI-*cb*-PS copolymer rod is about 4−6 nm, which is comparable to the unperturbed dimension (∼5.7 nm) of PS random coils[38] consisting of about 70 repeat units. As the stiffness of the FPI backbone is increased, the macromolecule assumes the shape of a rigid rod because of the increase in excluded volume arising from repulsion among the PS side chains.[39] The topographical scan of the surface with self-assembled macromolecular arrays in Figure 4a reveals well-defined repeating features of 6−7 nm in height. Thus, the side chains were present in a highly folded state, instead of in the fully extended conformation. The repeating features coincide with the macromolecular arrays, while the feature dimension is comparable to the lateral dimension of the comb-brush structure.

3.5. Thermal Stability, Processability, Mechanical Property, and Dielectric Constant of the Comb-Shaped Copolymers. Thermal stability, processability, mechanical property, and dielectric property are the main concerns for polymeric materials used as interlayer dielectrics in the new generation of submicron and nanolevel electronics.[24] When subjected to thermogravimetric analysis (TGA), the FPI macroinitiators underwent a two-step weight loss process. The first major weight loss at about 260 °C was probably associated with the decomposition of the bromoester groups. When heated to a temperature above 600 °C, about 50% of the weight remained. The phenomenon suggests that the FPI has been carbonized. The FPI-*cb*-PS and FPI-*cb*-PFS copolymers, on the other hand, underwent a clean major weight loss, commencing at about 400 and 470 °C, respectively. These temperatures corresponded to the thermal decomposition temperatures of the PS and PFS side chains. The results suggest that thermal stability of the copolymers is dominated by the PFS and PS brushes. Thus, the FPI-*cb*-PFS copolymer exhibits an excellent thermal stability owning to the presence

of fluorinated aromatic groups (see Figure S1, Supporting Information).

Both FPI-*cb*-PS and FPI-*cb*-PFS copolymers exhibit good solubility in common organic solvents, such as THF, DMF, and xylene. For example, 10 wt % THF solutions of FPI-*cb*-PS and FPI-*cb*-PFS2 can be prepared readily. Uniform FPI-*cb*-PS (and FPI-*cb*-PFS) films up to tens of microns in thickness can be obtained by spin-coating a 10 wt % THF solution of the copolymer at different rotation speeds. Thus, good solubility of the comb-shaped FPI-*cb*-PS and FPI-*cb*-PFS copolymers in common organic solvents has imparted good precessability to these copolymers with rigid backbones. The PFS homopolymer film is brittle. The film prepared from the PFS homopolymer, with a M_n of 2.7×10^4 g/mol and PDI of 1.12, has a tensile strength of about 0.6 MPa and a fracture strain of about 2−3%. In comparison, the FPI-*cb*-PFS copolymers have improved tensile strength of 0.9−1.1 MPa and fracture strain of about 5−7%, arising from the contribution of the PFI main chain and the entanglement of PFS side chains.

Dielectric constants (κ's) of the FPI film and the FPI-*cb*-PS and FPI-*cb*-PFS copolymer films are shown in Table 1. The FPI maroinitiator has a dielectric constant of about 3.0. For the FPI-*cb*-PS copolymers, relatively low dielectric constants (on the order of 2.6) were obtained. These κ values are comparable to that of the PS homopolymer.[40] The FPI-*cb*-PFS3 copolymer with a M_n of about 3.6×10^5 g/mol has a low dielectric constant of only about 2.1, which is lower than that of the PFS homopolymer ($\kappa \sim 2.2$)[41] and is comparable to that of the very inert poly(tetrafluoroethylene) ($\kappa \sim 2.1$).[42] This phenomenon can be accounted for by the fact that, in addition to having a high fluorine content, the copolymer with the comb-shaped macromolecular architecture had an increased free volume over those of the FPI and PFS homopolymers. The comb-shaped FPI-*cb*-PFS macromolecular architecture has a density of about 1.30 g/cm^3, which is lower than that of 1.43 g/cm^3 for the PFS homopolymer or that of 1.41 g/cm^3 for the FPI, arising probably from the less efficient packing of the rigid comb-shaped structure.

4. Conclusions

Comb-shaped FPI-*cb*-PS and FPI-*cb*-PFS copolymers were successfully prepared via ATRP of styrene and pentafluorostyrene, respectively, from the FPI-Br macroinitiators. The PS and PFS side chains in the comb-shaped copolymers were of well-defined lengths. The chain length of the PS and PFS side chains could be regulated by varying the ATRP time. The FPI-*cb*-PS copolymer with a M_n of about 9.4×10^3 g/mol, having about 14 fluorinated imide units in the rigid backbone (rod) and about 70 styrene units in each of the 14 side chains (coils), was shown to self-assemble into ordered arrays on the hydrogen-terminated (hydrophobic) silicon surface. The macromolecular assembly, consisting of aligned and uniformly spaced rigid rods of 20−30 nm in length and 4−6 nm in lateral dimension, was revealed by AFM images. In addition to good solution processability, the FPI-*cb*-PFS copolymer with its unique macromolecular architecture also exhibited good thermal stability, improved mechanical properties over those of the PFS homopolymer, and very low dielectric constant ($\kappa \sim 2.1$). The FPI-*cb*-PFS copolymer is thus a potential ultralow-κ material for submicron and nanolevel electronics.

Supporting Information Available: Thermal gravimetric analysis (TGA) curves for the PFI macroinitiators and the FPI-*cb*-PS and FPI-*cb*-PFS copolymers. This material is available free of charge via the Internet at http://pubs.acs.org.

References and Notes

(1) Ishizu, K.; Tusubaki, K.; Mori, A.; Uchida, S. *Prog. Polym. Sci.* **2003**, *28*, 27−54.
(2) Matyjaszewski, K. *ACS Symp. Ser.* **2003**, *854*, 2−9.
(3) Wang, A. R.; Zhu, S. P.; Matyjaszewski, K. *ACS Symp. Ser.* **2003**, *854*, 161−179.
(4) Pyun, J.; Matyjaszewski, K. *Chem. Mater.* **2001**, *13*, 3436−3448.
(5) Kotani, Y.; Kato, M.; Kamigaito, M.; Sawamoto, M. *Macromolecules* **1996**, *29*, 6979−6982.
(6) Davis, K. A.; Charleux, B.; Matyjaszewski, K. *J. Polym. Sci., Part A: Polym. Chem* **2000**, *38*, 2274−2283.
(7) Roos, S. G.; Müller, A. H. E.; Matyjaszewski, K. *Macromolecules* **1999**, *32*, 8331−8335.
(8) Mecerreyes, D.; Atthoff, B.; Boduch, K. A.; Trollsäs, M.; Hedrick, J. L. *Macromolecules* **1999**, *32*, 5175−5182.
(9) Baek, K.-Y.; Kamigaito, M.; Sawamoto, M. *Macromolecules* **2001**, *34*, 7629−7635.
(10) Du, J.-Z.; Chen, Y.-M. *Macromolecules* **2004**, *37*, 3588−3594.
(11) Switek, K. A.; Bates, F. S.; Hillmyer, M. A. *Macromolecules* **2004**, *37*, 6355−6361.
(12) Kotani, Y.; Kamigaito, M.; Sawamoto, M. *Macromolecules* **1998**, *31*, 5582−5587.
(13) Zhang, X.; Wang, P.; Zhu, P.; Ye, C.; Xi, F. *Macromol. Chem. Phys.* **2000**, *201*, 1853−1859.
(14) Haddleton, D. M.; Perrier, S.; Bon, S. A. F. *Macromolecules* **2000**, *33*, 8246−8251.
(15) Beers, K. L.; Gaynor, S. G.; Matyjaszewski, K. *Macromolecules* **1998**, *31*, 9413−9415.
(16) Kamigaito, M.; Ando, T.; Sawanmoto, M. *Chem. Rev.* **2001**, *101*, 3689−3745.
(17) Hawker, C. J.; Bosman, A. W.; Harth, E. *Chem. Rev.* **2001**, *101*, 3661−3688.
(18) Fischer, H. *J. Polym. Sci., Part A: Polym. Chem.* **1999**, *37*, 1885−1901.
(19) Yamada, K.; Miyazaki, M.; Ohno, K.; Fukuda, T.; Minoda, M. *Macromoleculaes* **1999**, *32*, 290−296.
(20) Zeng, F. Q.; Shen, Y. Q.; Zhu, S. P. *J. Polym. Sci., Part A: Polym. Chem.* **2002**, *40*, 2394−2405.
(21) Wang, X. S.; Armes, S. P. *Macromolecules* **2000**, *33*, 6640−6647.
(22) De Abajo, J.; de la Campa, J. G. In *Progress In Polyimide Chemistry I&II;* Kricheldorf, H. R., Ed.; Springer-Verlag: New York, 1999; p 24.
(23) Ohya, H.; Kudryyavtsev, V. V.; Semenova, S. I. *Polyimide membranes: Applications, Fabrications and Properties*; Kodansha Ltd.: Tokyo, Japan 1996; p 54.
(24) Maier, G. *Prog. Polym. Sci.* **2001**, *26*, 3−65.
(25) Miyagawa, T.; Fukushima, T.; Oyama, T.; Tomoi, M. *J. Polym. Sci., Part A: Polym. Chem.* **2003**, *41*, 861−871.
(26) Banerjee, S.; Madhra, M. K.; Salunke, A. K.; Jaiswal, D. K. *Polymer* **2003**, *44*, 613−620.
(27) Wang, W. C.; Vora, R. H.; Kang, E. T.; Neoh, K. G.; Ong, C. K.; Chen, L. F. *Adv. Mater.* **2004**, *16*, 54.
(28) Carter, K. R.; Dipietro, R. A.; Sanchez, M. I.; Swanson, S. A. *Chem. Mater.* **2001**, *13*, 213−221.
(29) Carter, K. R.; Dipietro, R. A.; Sanchez, M. I.; Russell, T. P.; Lakshmanan, P.; McGrath, J. E. *Chem. Mater.* **1997**, *9*, 105−118.
(30) Kang, D. W.; Kim, Y. M. *J. Inorg. Organomet. Polym.* **2002**, *12*, 79−165.
(31) EI Osaman, A.; Dumont, M. *Macromol. Symp.* **1999**, *137*, 137−142.
(32) Park, H. B.; Suh, I. Y.; Lee, Y. M. *Chem. Mater.* **2002**, *14*, 3034−3046.
(33) Coessens, V.; Pintauer, T.; Matyjaszewski, K. *Prog. Polym. Sci.* **2001**, *26*, 337−377.
(34) Zhang, Y.; Tan, K. L.; Liaw, B. Y.; Liaw, D. J.; Kang, E. T. *Thin Solid Films* **2000**, *374*, 70−76.
(35) Beamson, G.; Briggs, D. *High-Resolution XPS of Organic Polymers The scienta ESCA 300 Databse*; John Wiley & Sons: Chichester, England, 1992; p 274.

(36) Xu, F. J.; Yuan, Z. L.; Kang, E. T.; Neoh, K. G. *Langmuir* **2004**, *20*, 8200−2206.
(37) Simulation results using ACD Labs FreeWare 5.0, Advanced Chemistry Development Inc., Toronto, Canada.
(38) Billymer, F. W. *Texbook of Polymer Science*; Wiley-Interscience Publication: New York, 1984; p 178.
(39) Hadjichristidis, N.; Pitsikalis, M.; Iatrou, H.; Pispas, S. *Macromol. Rapid Commun.* **2003**, *24*, 979−992.
(40) Goodfellow Catalogue 2002, Goodfellow Inc., Cambridge, UK, p 78.
(41) Fu, G. D.; Yuan, Z. L.; Kang, E. T.; Neoh, K. G.; Lai, D. M. Y.; Huan, A. C. H. *Adv. Funct. Mater.* **2005**, *15*, 315−322.
(42) Kang, E. T.; Zhang, Y. *Adv. Mater.* **2000**, *12*, 1481−1494.

MA0506435